The Influence of Temperature on Ozone Production under varying NO_x Conditions – a modelling study

J. Coates[1], K. Mar[1], N. Ojha[2] and T. Butler[1]

[1]Institute for Advanced Sustainability Studies, Potsdam, Germany

[2]Max Planck Institute for Chemistry, Mainz, Germany

March 21, 2016

Abstract

Surface ozone is a secondary air pollutant produced during the degradation of emitted volatile organic compounds (VOCs) in the presence of sunlight and nitrogen oxides (NO_x). Temperature directly influences ozone production through speeding up the rates of the chemical reactions and increasing the emissions of VOCs, such as isoprene, from vegetation. In this study, we used a box model to examine the non-linear relationship between ozone, NO_x, and temperature and was compared to previous observational studies. Under high-NO_x conditions, an increase in ozone from 20 °C to 40 °C of up to 20 ppbv was due to faster reaction rates while increased isoprene emissions added up to a further 11 ppbv of ozone. The increased oxidation rate of emitted VOC with temperature controlled the rate of O_x production. The rate of increase in ozone mixing ratios with temperature from our box model simulations was about half the rate of increase in ozone with temperature observed over central Europe or simulated by a regional chemistry model. Modifying the box model setup to approximate stagnant conditions increased the rate of increase of ozone with temperature as the accumulation of oxidants enhanced ozone production through the increased production of peroxy radicals from the secondary degradation of emitted VOCs. The model simulations approximating stagnant conditions and VOC-and-NO_x-sensitive chemistry reproduced the 2 ppbv increase in ozone per °C from the observational and model data over central Europe. The simulated ozone-temperature relationship was more sensitive to mixing than the choice of chemical mechanism.

1

1 Introduction

Surface-level ozone (O_3) is a secondary air pollutant formed during the photochemical degradation of volatile organic compounds (VOCs) in the presence of nitrogen oxides ($NO_x \equiv NO + NO_2$). Due to the photochemical nature of ozone production, it is strongly influenced by meteorological variables such as temperature (Jacob and Winner, 2009). Otero et al. (2016) showed that temperature was a major meteorological driver for summertime ozone in many areas of central Europe.

Temperature primarily influences ozone production in two ways: speeding up the reaction rates of many chemical reactions, and increasing emissions of VOCs from biogenic sources (BVOCs) (Sillman and Samson, 1995). While emissions of anthropogenic VOCs (AVOCs) are generally not dependent on temperature, evaporative emissions of AVOCs increase with temperature (Rubin et al., 2006). The review of Pusede et al. (2015) provides further details of the temperature-dependent processes impacting ozone production.

Regional modelling studies over the US (Sillman and Samson, 1995; Steiner et al., 2006; Dawson et al., 2007) examined the sensitivity of ozone production during a pollution episode to increased temperatures. These studies noted that increased temperatures (without changing VOC or NO_x-conditions) led to higher ozone levels, often exceeding local air quality guidelines. Sillman and Samson (1995) and Dawson et al. (2007) varied the temperature dependence of the PAN (peroxy acetyl nitrate) decomposition rate during simulations of the eastern US determining the sensitivity of ozone production with temperature to the PAN decomposition rate. In addition to the influence of PAN decomposition on ozone production, Steiner et al. (2006) correlated the increase in ozone mixing ratios with temperature over California to increased mixing ratios of formaldehyde, a secondary degradation production of many VOC and an important radical source. Steiner et al. (2006) also noted increased emissions of BVOCs at higher temperatures in urban areas with high NO_x emissions also increased ozone levels with temperature.

Pusede et al. (2014) used an analytical model constrained by observations over the San Joaquin Valley, California to infer a non-linear relationship between ozone, temperature and NO_x, similar to the well-known non-linear relationship of ozone production on NO_x and VOC levels (Sillman, 1999). Moreover, Pusede et al. (2014) showed that temperature can be used as a surrogate for VOC levels when considering the relationship of ozone under different NO_x conditions.

Environmental chamber studies have also been used to analyse the relationship of ozone with temperature using a fixed mixture of VOCs. The chamber experiments of Carter et al. (1979) and Hatakeyama et al. (1991) showed increases in ozone from a VOC mix with temperature. Both studies compared the concentration time series of ozone and nitrogen-containing compounds (NO_x, PAN, HNO_3) at various temperatures linking the maximum ozone concentration to the decrease in PAN concentrations at temperatures greater than 303 K.

Despite many studies considering the ozone-temperature relationship from an observational and chamber study perspective, modelling studies focusing on the detailed chemical processes of the ozone-temperature relationship under different NO_x conditions have not been performed (to our knowledge). The regional modelling studies described previously concentrated on reproducing ozone levels (using a single chemical mechanism) over regions with known meteorology and NO_x conditions then varying the temperature. These modelling studies did not consider the relationship between ozone, NO_x and temperature. The review of Pusede et al. (2015) also highlights a lack of modelling studies looking at the relationship of ozone with temperature under different NO_x conditions.

Comparisons of different chemical mechanisms, such as Emmerson and Evans (2009) and Coates and Butler (2015), showed that different representations of tropospheric chemistry influenced ozone production. Neither of these studies examined the ozone-temperature relationship differences between chemical mechanisms. Furthermore, Rasmussen et al. (2013) acknowledged that the modelled ozone-temperature relationship may be sensitive to the choice of chemical mechanism and recommended investigating this sensitivity. Comparing the ozone-temperature relationship predicted by different chemical mechanisms is potentially important for modelling of future air quality due to the expected increase in heatwaves (Karl and Trenberth, 2003).

In this study, we use an idealised box model to determine how ozone levels vary with temperature under different NO_x conditions. We determine whether faster chemical reaction rates or increased BVOC emissions have a greater influence on instantaneous ozone production with higher temperature under different NO_x conditions. Furthermore, we compare the ozone-temperature relationship produced by different chemical mechanisms.

2 Methodology

2.1 Model Setup

We used the MECCA box model (Sander et al., 2005) to determine the important gas-phase chemical processes for ozone production under different temperatures and NO_x conditions. The MECCA box model was set up as described in Coates and Butler (2015) and updated to include vertical mixing with the free troposphere using a diurnal cycle for the PBL height. The supplementary material includes further details of these updates.

Simulations broadly representative of urban conditions in central Europe. The simulations started at 06:00 with a total run time of two days. Methane was fixed at 1.7 ppmv throughout the model run, carbon monoxide (CO) and ozone were initialised at 200 ppbv and 40 ppbv and then allowed to evolve freely throughout the simulation. All VOC emissions were held constant until noon of first day simulating a plume of freshly-emitted VOC.

Separate box model simulations were performed by systematically varying the temperature between 288 and 313 K (15 – 40 °C) in steps of 0.5 K. NO emissions were systematically varied between 5.0×10^9 and 1.5×10^{12} molecules(NO) cm^{-2} s^{-1} in steps of 1×10^{10} molecules(NO) cm^{-2} s^{-1} at each temperature. At 20 °C, these NO emissions corresponded to peak NO_x mixing ratios of 0.02 ppbv and 10 ppbv respectively, this range of NO_x mixing ratios covers the NO_x conditions found in pristine and urban conditions (von Schneidemesser et al., 2015).

All simulations were repeated using different chemical mechanisms to investigate whether the relationship between ozone, temperature and NO_x changes using different representations of ozone production chemistry. The reference chemical mechanism was the near-explicit Master Chemical Mechanism, MCMv3.2, (Jenkin et al., 1997, 2003; Saunders et al., 2003; Rickard et al., 2015). The reduced chemical mechanisms in our study were Common Representative Intermediates, CRIv2 (Jenkin et al., 2008), Model for OZone and Related Chemical Tracers, MOZART-4 (Emmons et al., 2010), Regional Acid Deposition Model, RADM2 (Stockwell et al., 1990) and the Carbon Bond Mechanism, CB05 (Yarwood et al., 2005). Coates and Butler (2015) described the implementation of these chemical mechanisms in MECCA. These reduced chemical mechanisms were chosen as they are commonly used by modelling groups in 3D regional and global models (Baklanov et al., 2014).

Model runs were repeated using a temperature-dependent and temperature-independent

Table 1: Total AVOC emissions in 2011 in tonnes from each anthropogenic source category assigned from TNO-MACC_III emission inventory and temperature-independent BVOC emissions in tonnes from Benelux region assigned from EMEP. The allocation of these emissions to MCMv3.2, CRIv2, CB05, MOZART-4 and RADM2 species are found in the supplementary material.

Source Category	Total Emissions	Source Category	Total Emissions
Public Power	13755	Road Transport: Diesel	6727
Residential Combustion	21251	Road Transport: Others	1433
Industry	62648	Road Transport: Evaporation	2327
Fossil Fuel	15542	Non-road Transport	17158
Solvent Use	100826	Waste	1342
Road Transport: Gasoline	24921	BVOC	10702

source of BVOC emissions to determine the relative importance of increased emissions of BVOC and faster reaction rates of chemical processes for the increase of ozone with temperature. MEGAN2.1 (Guenther et al., 2012) specified the temperature-dependent BVOC emissions of isoprene, Sect. 2.3 provides further details. As isoprene emissions are the most important on the global scale (Guenther et al., 2006), we considered only isoprene emissions from vegetation. Only isoprene emissions were dependent on temperature, all other emissions were constant in all simulations. In reality, many other BVOC are emitted from varying vegetation types (Guenther et al., 2006) and increased temperature can also increase AVOC emissions through increased evaporation (Rubin et al., 2006).
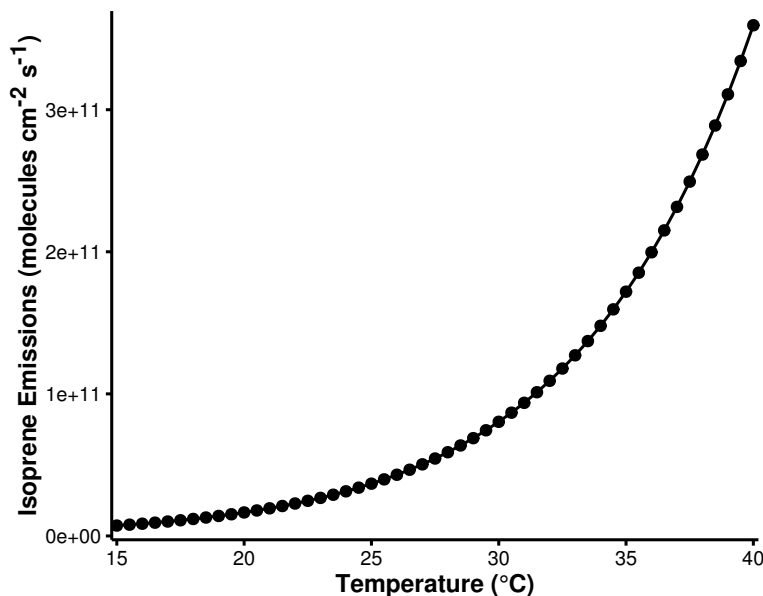
2.2 VOC Emissions

Emissions of urban AVOC over central Europe were taken from TNO-MACC_III emission inventory for the Benelux (Belgium, Netherlands and Luxembourg) region for the year 2011. TNO-MACC_III is the updated TNO-MACC_II emission inventory created using the same methodology as Kuenen et al. (2014) and based upon improvements to the existing emission inventory during AQMEII-2 (Pouliot et al., 2015).

Temperature-independent emissions of isoprene and monoterpenes from biogenic sources were calculated as a fraction of the total AVOC emissions from each country in the Benelux region. This data was obtained from the supplementary data available from the EMEP (European Monitoring and Evaluation Programme) model (Simpson et al., 2012). Temperature-dependent emissions of isoprene are detailed in Sect. 2.3.

Table 1 shows the quantity of VOC emissions from each source category and the

Figure 1: The estimated isoprene emissions (molecules isoprene cm^{-2} s^{-1}) using MEGAN2.1 at each temperature used in the study.

temperature-independent BVOC emissions. These AVOC emissions were assigned to chemical species and groups based on the profiles provided by TNO. The NMVOC emissions were speciated to MCMv3.2 species as described by von Schneidemesser et al. (2016). For simulations done with other chemical mechanisms, the VOC emissions represented by the MCMv3.2 were mapped to the mechanism species representing VOC emissions in each reduced chemical mechanism based on the recommendations of the source literature and Carter (2015). The VOC emissions in the reduced chemical mechanisms were weighted by the carbon numbers of the MCMv3.2 species and the emitted mechanism species, thus keeping the amount of emitted reactive carbon constant between simulations. The supplementary data outlines the primary VOC and calculated emissions with each chemical mechanism.

2.3 Temperature Dependent Isoprene Emissions

Temperature-dependent emissions of isoprene were estimated using the MEGAN2.1 algorithm for calculating the emissions of VOC from vegetation (Guenther et al., 2012). Emissions from nature are dependent on many variables including temperature, radiation and age but for the purpose of our study all variables except temperature were held constant.

The MEGAN2.1 parameters were chosen to give similar isoprene mixing ratios at 20 °C to the temperature-independent emissions of isoprene in order to compare the effects of increased isoprene emissions with temperature. The estimated emissions of isoprene with MEGAN2.1

Table 2: Increase in mean ozone mixing ratio (ppbv) due to chemistry (i.e. faster reaction rates) and temperature-dependent isoprene emissions from 20 °C to 40 °C in the NO_x-regimes of Fig. 3.

Chemical Mechanism	Source of Difference	Increase in Ozone from 20 °C to 40 °C (ppbv)		
		Low-NO_x	Maximal-O_3	High-NO_x
MCMv3.2	Isoprene Emissions	4.6	7.7	10.6
	Chemistry	6.8	12.5	15.2
CRIv2	Isoprene Emissions	4.8	7.9	10.8
	Chemistry	6.0	11.1	13.7
MOZART-4	Isoprene Emissions	4.1	6.7	10.0
	Chemistry	6.0	10.2	12.3
CB05	Isoprene Emissions	4.6	7.4	9.8
	Chemistry	9.3	16.0	19.9
RADM2	Isoprene Emissions	3.8	5.7	7.8
	Chemistry	8.6	14.1	17.3

using these assumptions are illustrated in Fig. 1 and show the expected exponential increase in isoprene emissions with temperature (Guenther et al., 2006).

The estimated emissions of isoprene at 20 °C lead to 0.07 ppbv of isoprene in our simulations while at 30 °C, the increased emissions of isoprene using MEGAN2.1 estimations lead to 0.35 ppbv of isoprene in the model. A measurement campaign over Essen, Germany (Wagner and Kuttler, 2014) measured 0.1 ppbv of isoprene at temperature 20 °C and 0.3 ppbv of isoprene were measured at 30 °C. The similarity of the simulated and observed isoprene mixing ratios indicates that the MEGAN2.1 variables chosen for calculating the temperature-dependent emissions of isoprene were suitable for simulating urban conditions over central Europe.

3 Results and Discussion

3.1 Relationship between Ozone, NO_x and Temperature

Figure 2 depicts the peak mixing ratio from ozone of each simulation as a function of the total NO_x emissions and temperature on the first day of simulations when using a temperature-independent and temperature-dependent source of isoprene emissions for each chemical mechanism. A non-linear relationship of ozone mixing ratios with NO_x and temperature is produced by each chemical mechanism. This non-linear relationship is similar to that determined by Pusede et al. (2014) using an analytical model constrained to observational measurements over the San Joaquin Valley, California.

Higher peak ozone mixing ratios are produced when using a temperature-dependent source of isoprene emissions (Fig. 2). The highest mixing ratios of peak ozone are produced at high temperatures and moderate emissions of NO_x regardless of the temperature dependence of

Figure 2: Contours of peak ozone mixing ratios (ppbv) as a function of the total NO_x emissions on the first day and temperature for each chemical mechanism using a temperature-dependent and temperature-independent source of isoprene emissions. The contours can be split into three separate regimes: High-NO_x, Maximal-O_3 and Low-NO_x indicated in the figure.
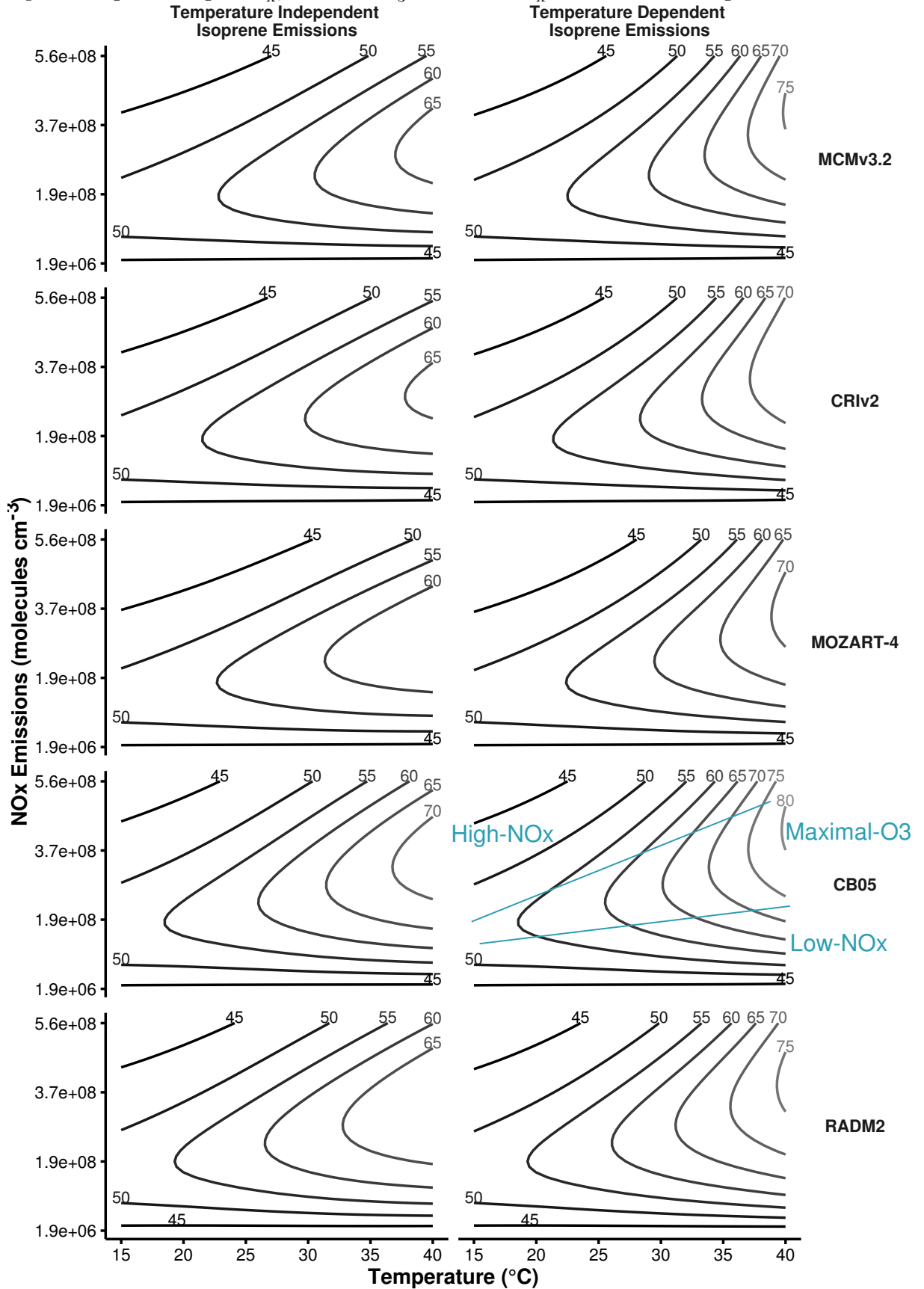
Figure 3: Mean ozone mixing ratios (ppbv) at each temperature after allocation to the different NO_x-regimes of Fig. 2. The differences in ozone mixing ratios due to chemistry (solid line) and isoprene emissions (dotted line) are represented graphically for MOZART-4 with High-NO_x conditions. Table 2 details the differences for each chemical mechanism and NO_x-condition.
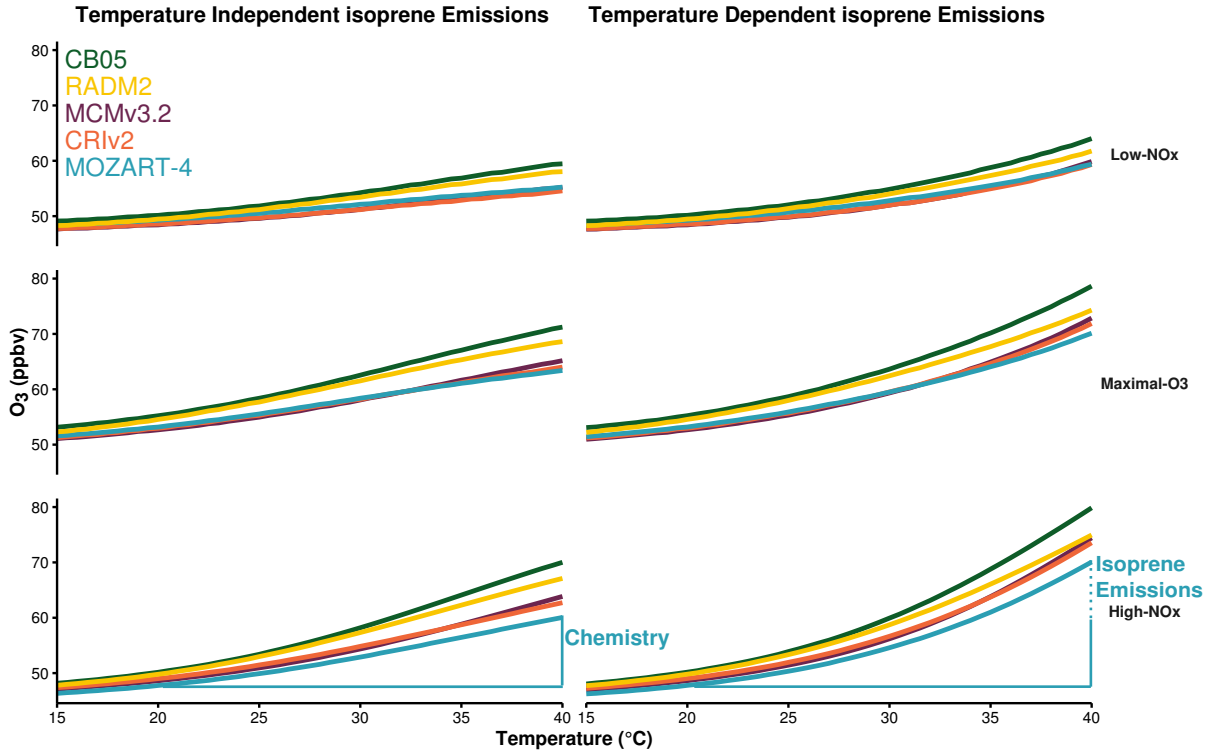
isoprene emissions. Conversely, the least amount of peak ozone is produced with low emissions of NO_x over the whole temperature range (15 – 40 °C) when using both a temperature-independent and temperature-dependent source of isoprene emissions.

The contours of ozone mixing ratios as a function of NO_x and temperature can be split into three NO_x regimes (Low-NO_x, Maximal-O_3 and High-NO_x), similar to the NO_x regimes defined for the non-linear relationship of ozone with VOC and NO_x. The Low-NO_x regime corresponds with regions having little increase in ozone with temperature, also called the NO_x-sensitive regime. The High-NO_x (or NO_x-saturated) regime is when ozone levels increase rapidly with temperature. The contour ridges correspond to regions of maximal ozone production; this is the Maximal-O_3 regime. Pusede et al. (2014) showed that temperature can be used as a proxy for VOC, thus we assigned the ozone mixing ratios from each box model simulation to a NO_x regime based on the ratio of HNO_3 to H_2O_2. This ratio was used by Sillman (1995) to designate ozone to NO_x regimes based on NO_x and VOC levels. The Low-NO_x regime corresponds to H_2O_2:HNO_3 ratios less than 0.5, the High-NO_x regime corresponds to ratios larger than 0.3 and ratios between 0.3 and 0.5 correspond to the Maximal-O3 regime.

The peak ozone mixing ratio from each simulation was assigned to a NO_x regime based on the H_2O_2:HNO_3 ratio of that simulation. The peak ozone mixing ratios assigned to each NO_x regime at each temperature were averaged, and illustrated in Figure 3 for each chemical mechanism and each type of isoprene emissions (temperature independent and temperature dependent). We define the absolute increase in ozone from 20 °C to 40 °C due to faster reaction rates as the difference between ozone mixing ratios from 20 °C to 40 °C when using a temperature-independent source of isoprene emissions. When using a temperature-dependent source of isoprene emissions, the difference in ozone mixing ratios from 20 °C to 40 °C minus the increase due to faster reaction rates, gives the absolute increase in ozone mixing ratios from increased isoprene emissions. These differences are represented graphically in Fig. 3 and summarised in Table 2.

Table 2 shows that the absolute increase in ozone with temperature due to chemistry (i.e. faster reaction rates) is larger than the absolute increase in ozone due to increased isoprene emissions for each chemical mechanism and each NO_x regime. In all cases the absolute increase in ozone is largest under High-NO_x conditions and lowest with Low-NO_x conditions (Fig. 3 and Table 2). The increase in ozone mixing ratio from 20 °C to 40 °C due to faster reaction rates with High-NO_x conditions is almost double that with Low-NO_x conditions. In the Low-NO_x regime, the increase of ozone with temperature using the reduced chemical mechanisms (CRIv2, MOZART-4, CB05 and RADM2) is similar to that from the MCMv3.2. Larger differences occur in the Maximal-O_3 and High-NO_x regimes.

All reduced chemical mechanisms except RADM2 have similar increases in ozone due to increased isoprene emissions as the MCMv3.2 (Table 2). RADM2 produces 3 ppbv less ozone than the MCMv3.2 due to increased isoprene emissions in each NO_x regime, indicating that this difference is due the representation of isoprene degradation chemistry in RADM2.

The Tagged Ozone Production Potential (TOPP) defined in Butler et al. (2011) is a measure of the number of molecules of ozone produced per molecule of VOC emitted. Coates and Butler (2015) compared ozone production in different chemical mechanisms to the MCMv3.2 using TOPPs and showed that less ozone is produced per molecule of isoprene emitted using RADM2 than with MCMv3.2. The degradation of isoprene has been extensively studied and it is well-known that methyl vinyl ketone (MVK) and methacrolein are signatures of isoprene degradation (Atkinson, 2000). All chemical mechanisms in our study except RADM2 explicitly represent MVK and methacrolein (or in the case of CB05, a lumped species representing both these secondary degradation products). RADM2 does not represent methacrolein and the

10

Figure 4: Day-time budgets of O_x normalised by the total loss rate of emitted VOC in the NO_x-regimes of Fig. 3. The white line indicates net production or consumption of O_x. The net contribution of reactions to O_x budgets are allocated to categories of deposition, inorganic reactions, peroxy nitrates (RO2NO2), reactions of NO with HO2, alkyl peroxy radicals (RO2) and acyl peroxy radicals (ARO2). All other reactions are allocated to the 'Other Organic' category.
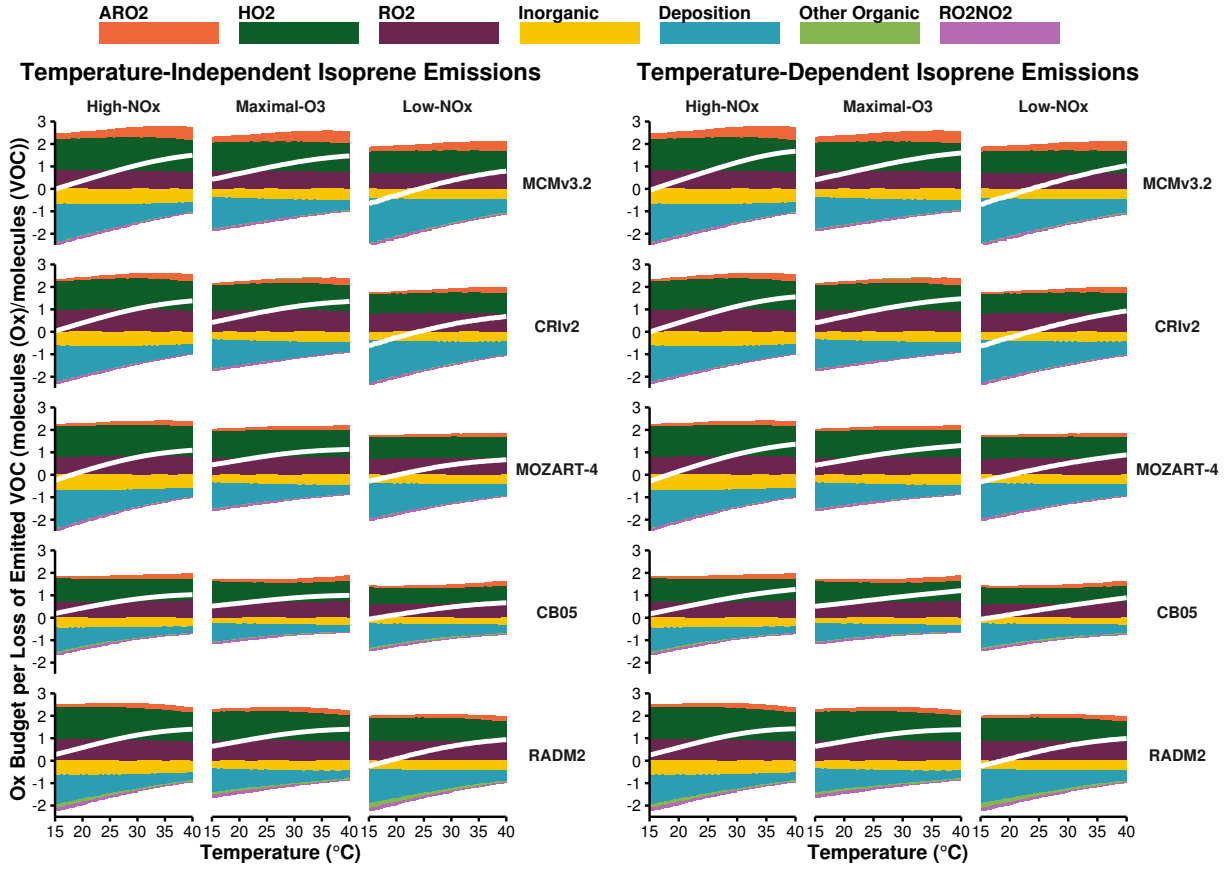
mechanism species representing ketones (KET) is a mixture of acetone and methyl ethyl ketone (MEK) (Stockwell et al., 1990). Thus the secondary degradation of isoprene in RADM2 is unable to represent the ozone production from the further degradation of the signature secondary degradation products of isoprene, MVK and methacrolein. Updated versions of RADM2, RACM (Stockwell et al., 1997) and RACM2 (Goliff et al., 2013), sequentially included methacrolein and MVK and with these updates the TOPP value of isoprene approached that of the MCMv3.2 (Coates and Butler, 2015).

3.2 Ozone Production and Consumption Budgets

In order to understand the temperature dependence of ozone production directly, we examine the day-time production and consumption budgets of O_x ($\equiv O_3 + NO_2 + O(^1D) + O$) normalised by the total loss rate of the emitted VOC (Fig. 4). The O_x budgets are assigned to each NO_x regime for each chemical mechanism and type of isoprene emissions. The budgets are allocated to the net contribution of major categories, where 'HO2', 'RO2', 'ARO2' represent the reactions of NO

with HO_2, alkyl peroxy radicals and acyl peroxy radicals respectively. 'RO2NO2' represents the net effects of peroxy nitrates, 'Deposition' represents ozone deposition, 'Inorganic' is all other inorganic contributions to O_x production. Any other remaining organic reactions are included in the 'Other Organic' category. Figure 4 also illustrates the net production or consumption of O_x in each case. The ratio of net ozone to net O_x production was practically constant with temperature in all cases showing that using O_x budgets as a proxy for ozone budgets was suitable at each temperature in our study.

The net O_x production efficiency increases from 20 °C to 40 °C by ~ 1 molecule of O_x per molecule of VOC oxidised with each chemical mechanism, NO_x-condition and type of isoprene emissions (Fig. 4). The net O_x production per oxidation of emitted VOC increases with temperature due to a decrease in ozone deposition per molecule of VOC oxidation with temperature. Ozone deposition is treated as a temperature-independent process in the boxmodel but in reality, deposition of ozone to vegetation is influenced by temperature with the temperature dependence of ozone deposition varying between vegetation types (Mészáros et al., 2009). Representing the temperature dependence of ozone deposition to vegetation is relevant for areas rich in vegetation but less so for the urban conditions simulated in our box model.

As the production efficiency of O_x remains constant with temperature (~ 2 molecules of O_x per molecule of VOC oxidised, Fig. 4), the rate of O_x production is controlled by the oxidation of VOCs. Faster oxidation of VOCs with temperature speeds up the production of peroxy radicals increasing ozone production when peroxy radicals react with NO to produce NO_2. The reactivity of VOCs has been linked to ozone production (e.g. Kleinman (2005), Sadanaga et al. (2005)) and the review of Pusede et al. (2015) acknowledged the importance of organic reactivity and radical production to the ozone-temperature relationship. Also, the modelling study of Steiner et al. (2006) noted that the increase in initial oxidation rates of VOCs with temperature leads to increased formaldehyde concentrations and in turn an increase of ozone as formaldehyde is an important source of HO_2 radicals.

Increased VOC oxidation with temperature is tied to faster reaction rates and increased levels of OH with temperature. An increase of ozone with temperature goes hand in hand with an increase of OH with temperature since ozone photolysis is the dominant source of OH radicals in the atmosphere.

$$O_3 + h\nu \rightarrow O(^1D) + O_2 \tag{R1}$$

$$O(^1D) + H_2O \rightarrow OH + OH \tag{R2}$$

Table 3: Slopes ($m_{O3\text{-}T}$, ppbv per °C) of the linear fit to MDA8 values of ozone and temperature correlations in Fig. 5, indicating the increase of MDA8 in ppbv of ozone per °C. The slope of the observational data is 2.15 ppbv/°C and the slope of the WRF-Chem output is 2.05 ppbv/°C.

Mechanism	Isoprene Emissions	Low-NO$_x$		Maximal-O$_3$		High-NO$_x$	
		Mixing	No Mixing	Mixing	No Mixing	Mixing	No Mixing
MCMv3.2	Temperature Independent	0.28	1.01	0.51	1.36	0.59	0.96
	Temperature Dependent	0.42	1.48	0.74	2.16	0.93	2.63
CRIv2	Temperature Independent	0.25	0.93	0.47	1.27	0.55	0.88
	Temperature Dependent	0.40	1.44	0.71	2.09	0.90	2.52
MOZART-4	Temperature Independent	0.25	0.97	0.44	1.21	0.49	0.59
	Temperature Dependent	0.38	1.43	0.65	1.98	0.81	2.05
CB05	Temperature Independent	0.39	1.30	0.67	1.72	0.79	1.45
	Temperature Dependent	0.52	1.72	0.89	2.44	1.12	2.94
RADM2	Temperature Independent	0.37	1.31	0.61	1.64	0.70	1.28
	Temperature Dependent	0.48	1.68	0.79	2.22	0.97	2.49

Furthermore, enhanced formaldehyde production from the faster degradation of VOCs increases HO$_2$ formation speeding up the reaction rate of the reaction of HO$_2$ and NO. (R3) is responsible for both ozone production (through NO$_2$ production) and OH recycling illustrating the strong coupling of ozone and OH production.

$$HO_2 + NO \rightarrow NO_2 + OH \tag{R3}$$

The net effect of peroxy nitrates on O$_x$ budgets in our study is negligible, contributing to a loss of ~ 0.1 molecules of O$_x$ per VOC oxidised from 20 °C to 40 °C (Fig. 4). Peroxy nitrates are produced from the reactions of acyl peroxy radicals with NO$_2$ and are an important reservoir of peroxy radicals and NO$_x$. The decomposition rate of peroxy nitrates is strongly temperature dependent and at higher temperatures the faster decomposition rate of RO$_2$NO$_2$ leads to faster release of peroxy radicals and NO$_2$. Dawson et al. (2007) attributed the increase in maximum 8 h ozone mixing ratios with temperature during a modelling study over the eastern US to the decrease in PAN lifetime with temperature. Steiner et al. (2006) also recognised that the decrease in PAN lifetime with temperature contributed to the increase of ozone with temperature concluding that the combined effects of increased oxidation rates of VOC and faster PAN decomposition increased the production of ozone with temperature. In our results (Fig. 4), the net effect of RO$_2$NO$_2$ is small since the decomposition rate is almost exactly balanced by the production from RO$_2$ + NO$_2$.

3.3 Comparison to Observations and 3D Model Simulations

This section compares the results from our idealised box model simulations to real-world observations and model output from a 3D model. Otero et al. (2016) showed that over the

Figure 5: MDA8 values of ozone from the box model simulations allocated to the different NO$_x$ regimes for each chemical mechanism with mixing (solid lines) and without mixing (dashed lines). The box model ozone-temperature correlation is compared to the summer 2007 observational data (black circles) and WRF-Chem output (purple boxes).
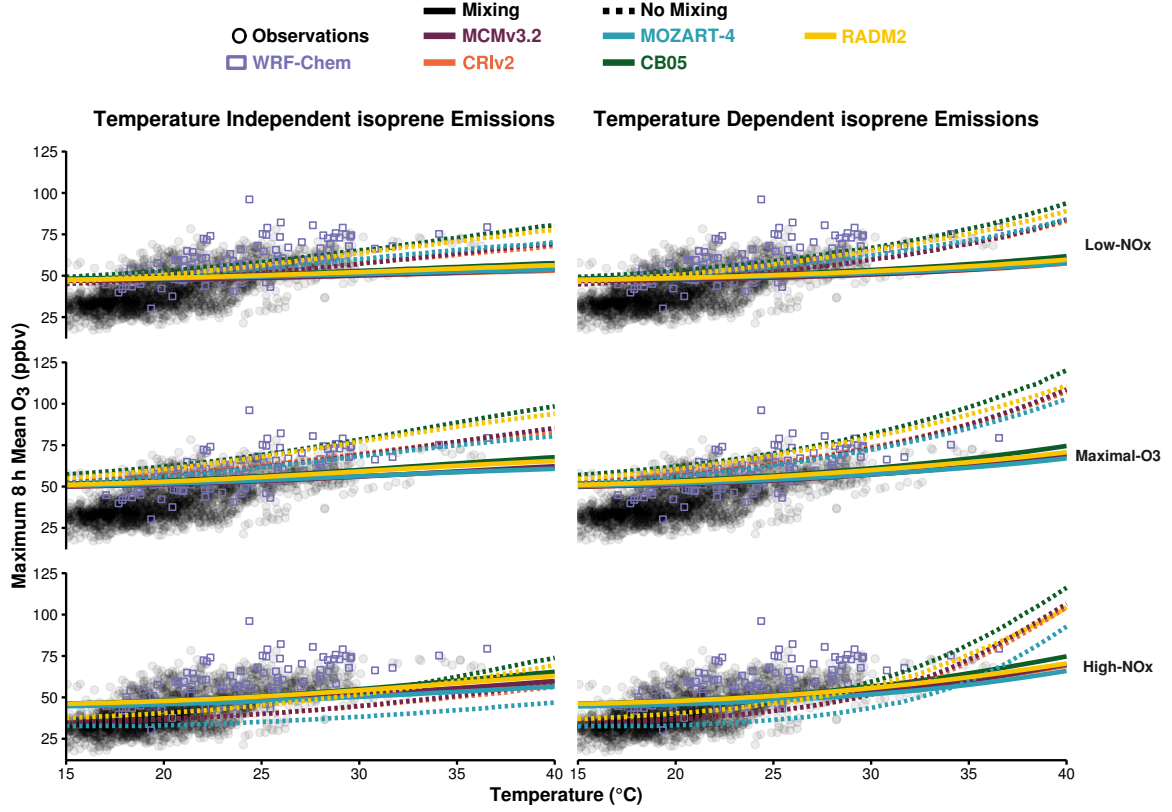
summer (JJA) months, temperature is the main meteorological driver of ozone production over many regions of central Europe using the interpolated observations of the maximum daily 8 h mean (MDA8) of ozone from Schnell et al. (2015) and the meteorological observational data set of the ERA-Interim re-analysis. Model output from the 3D WRF-Chem regional model using MOZART-4 chemistry set-up over the European domain for simulations of the year 2007 from Mar et al. (2016) was used to further compare the box model simulations to a model including more meteorological processes than our box model.

Figure 5 compares the observational and WRF-Chem data from summer 2007 over central and eastern Germany, where summertime ozone values are driven by temperature (Otero et al., 2016), to the MDA8 values of ozone from the box model simulations for each chemical mechanism. Despite, a high bias in simulated ozone in WRF-Chem, the rate of change of ozone with temperature from the WRF-Chem simulations (2.05 ppbv/°C) is similar to the rate of change of ozone with temperature from the observed data (2.15 ppbv/°C). The differences in ozone production between the different chemical mechanisms with the box model are small compared to the spread of the observational and WRF-Chem data. A temperature-dependent source of

14

isoprene with high-NO$_x$ conditions produces the most similar ozone-temperature slope to the observational data but lower than the observed ozone-temperature slope by a factor of two. In particular, the box model simulations over-predict the ozone values at lower temperatures and under-predict the ozone values at higher temperatures compared to the observed data.

Table 3 summarises the slopes (m$_{O3-T}$) of the linear fits of the box model simulations displayed in Fig. 5 in ppbv of ozone per °C determining the rate of increase of ozone with temperature. The main reason for the box model simulations being less sensitive to temperature than the observations and WRF-Chem is related to the set-up of the box model. In our simulations, we focused on instantaneous production of ozone from a freshly-emitted source of VOC with transport of the chemical species into the free troposphere. This box model setup did not consider stagnant atmospheric conditions characterised by low wind speeds slowing the transport of ozone and its precursors away from sources. Stagnant conditions have been correlated to high-ozone episodes in the summer over eastern US (Jacob et al., 1993).

In order to investigate the sensitivity of ozone production to mixing, box model simulations were performed without vertical mixing to approximate stagnant conditions that favour oxidant accumulation. The ozone-temperature relationship obtained with each chemical mechanism, using both a temperature-independent and temperature-dependent source of isoprene emissions and the different NO$_x$ conditions are displayed in Fig. 5. The rate of increase with ozone with temperature from these box model simulations are also included in Table 3.

In each case, the rate of increase of ozone with temperature increased in the box model simulations without mixing. The m$_{O3-T}$ calculated from the box model simulations without mixing using a temperature-dependent source of isoprene and with Maximal-O3 conditions (ranging between 2.0 and 2.4 ppbv/°C) are the very similar to the slopes of the observational and WRF-Chem results (2.1 and 2.2 ppbv/°C, respectively). The differences in m$_{O3-T}$ when not including mixing in the box model compared to the differences in m$_{O3-T}$ between chemical mechanisms in Table 3 show that the ozone-temperature relationship using our box model setup is more sensitive to mixing than the choice of chemical mechanism.

When approximating stagnant conditions with the box model, the oxidation rates of VOC and the secondary degradation products increased leading to increased ozone production compared to the simulations including mixing. Furthermore, in the model simulations without mixing, the secondary degradation of the VOCs was allowed to fully evolve increasing the production of peroxy radicals which produce ozone when reacting with NO. Similar to the results in Sect. 3.2,

the increase in the net normalised O_x production in the model simulations without mixing was controlled by the decrease in ozone deposition per molecule of VOC oxidised and the net contribution of peroxy nitrates was negligible.

4   Conclusions

In this study, we determined the effects of temperature on ozone production using a box model over a range of temperatures and NO_x conditions with a temperature-independent and temperature-dependent source of isoprene emissions. These simulations were repeated using reduced chemical mechanism schemes (CRIv2, MOZART-4, CB05 and RADM2) typically used in 3D models and compared to the near-explicit MCMv3.2 chemical mechanism.

Each chemical mechanism produced a non-linear relationship of ozone with temperature and NO_x with the most ozone produced at high temperatures and moderate emissions of NO_x. Conversely, lower NO_x levels led to a minimal increase of ozone with temperature. Thus air quality in a future with higher temperatures would benefit from dramatical reductions in NO_x emissions.

Faster reaction rates at higher temperatures were responsible for a greater absolute increase in ozone than increased isoprene emissions. In our simulations, ozone production was controlled by the increased rate of VOC oxidation with temperature. The net production of O_x per oxidised molecule of emitted VOC with temperature was regulated by the decrease of ozone deposition per molecule of emitted VOC oxidised.

The rate of increase of ozone with temperature using observational data over Europe was twice as high as the rate of increase of ozone with temperature when using the box model. This was consistent with our box model setup not representing stagnant atmospheric conditions that are inherently included in observational data and models including meteorology, such as WRF-Chem. Model simulations without mixing determined the sensitivity of the ozone-temperature relationship to mixing and in these model runs the rate of increase of ozone with temperature was faster than the simulations including mixing. The simulations without mixing with VOC-and-NO_x sensitive chemistry led to very similar rates of increase of ozone with temperature to the observational and WRF-Chem data. Furthermore, the ozone-temperature relationship was more sensitive to mixing than the choice of chemical mechanism.

16

Acknowledgements

References

R. Atkinson. Atmospheric chemistry of VOCs and NO$_x$. *Atmospheric Environment*, 34(12-14): 2063–2101, 2000.

A. Baklanov, K. Schlünzen, P. Suppan, J. Baldasano, D. Brunner, S. Aksoyoglu, G. Carmichael, J. Douros, J. Flemming, R. Forkel, S. Galmarini, M. Gauss, G. Grell, M. Hirtl, S. Joffre, O. Jorba, E. Kaas, M. Kaasik, G. Kallos, X. Kong, U. Korsholm, A. Kurganskiy, J. Kushta, U. Lohmann, A. Mahura, A. Manders-Groot, A. Maurizi, N. Moussiopoulos, S. T. Rao, N. Savage, C. Seigneur, R. S. Sokhi, E. Solazzo, S. Solomos, B. Sørensen, G. Tsegas, E. Vignati, B. Vogel, and Y. Zhang. Online coupled regional meteorology chemistry models in Europe: current status and prospects. *Atmospheric Chemistry and Physics*, 14(1):317–398, 2014.

T. Butler, M. Lawrence, D. Taraborrelli, and J. Lelieveld. Multi-day ozone production potential of volatile organic compounds calculated with a tagging approach. *Atmospheric Environment*, 45 (24):4082 – 4090, 2011.

W. P. L. Carter. Development of a Database for Chemical Mechanism Assignments for Volatile Organic Emissions. *Journal of the Air & Waste Management Association*, 0, 2015.

W. P. L. Carter, A. M. Winer, K. R. Darnall, and J. N. P. Jr. Smog chamber studies of temperature effects in photochemical smog. *Environmental Science & Technology*, 13(9):1094–1100, 1979.

J. Coates and T. M. Butler. A comparison of chemical mechanisms using tagged ozone production potential (TOPP) analysis. *Atmospheric Chemistry and Physics*, 15(15):8795–8808, 2015.

J. P. Dawson, P. J. Adams, and S. N. Pandis. Sensitivity of ozone to summertime climate in the eastern USA: A modeling case study . *Atmospheric Environment*, 41(7):1494 – 1511, 2007.

K. M. Emmerson and M. J. Evans. Comparison of tropospheric gas-phase chemistry schemes for use within global models. *Atmospheric Chemistry and Physics*, 9(5):1831–1845, 2009.

L. K. Emmons, S. Walters, P. G. Hess, J.-F. Lamarque, G. G. Pfister, D. Fillmore, C. Granier, A. Guenther, D. Kinnison, T. Laepple, J. Orlando, X. Tie, G. Tyndall, C. Wiedinmyer, S. L.

Baughcum, and S. Kloster. Description and evaluation of the Model for Ozone and Related chemical Tracers, version 4 (MOZART-4). *Geoscientific Model Development*, 3(1):43–67, 2010.

W. S. Goliff, W. R. Stockwell, and C. V. Lawson. The regional atmospheric chemistry mechanism, version 2. *Atmospheric Environment*, 68:174 – 185, 2013.

A. Guenther, T. Karl, P. Harley, C. Wiedinmyer, P. I. Palmer, and C. Geron. Estimates of global terrestrial isoprene emissions using MEGAN (Model of Emissions of Gases and Aerosols from Nature). *Atmospheric Chemistry and Physics*, 6(11):3181–3210, 2006.

A. B. Guenther, X. Jiang, C. L. Heald, T. Sakulyanontvittaya, T. Duhl, L. K. Emmons, and X. Wang. The Model of Emissions of Gases and Aerosols from Nature version 2.1 (MEGAN2.1): an extended and updated framework for modeling biogenic emissions. *Geoscientific Model Development*, 5(6):1471–1492, 2012.

S. Hatakeyama, H. Akimoto, and N. Washida. Effect of temperature on the formation of photochemical ozone in a propene-nitrogen oxide (NOx)-air-irradiation system. *Environmental Science & Technology*, 25(11):1884–1890, 1991.

D. J. Jacob and D. A. Winner. Effect of climate change on air quality. *Atmospheric Environment*, 43(1):51 – 63, 2009. Atmospheric Environment - Fifty Years of Endeavour.

D. J. Jacob, J. A. Logan, G. M. Gardner, R. M. Yevich, C. M. Spivakovsky, S. C. Wofsy, S. Sillman, and M. J. Prather. Factors regulating ozone over the United States and its export to the global atmosphere. *Journal of Geophysical Research*, 98(D8), 1993.

M. Jenkin, L. Watson, S. Utembe, and D. Shallcross. A Common Representative Intermediates (CRI) mechanism for VOC degradation. Part 1: Gas phase mechanism development. *Atmospheric Environment*, 42(31):7185 – 7195, 2008.

M. E. Jenkin, S. M. Saunders, and M. J. Pilling. The tropospheric degradation of volatile organic compounds: a protocol for mechanism development. *Atmospheric Environment*, 31(1):81 – 104, 1997.

M. E. Jenkin, S. M. Saunders, V. Wagner, and M. J. Pilling. Protocol for the development of the Master Chemical Mechanism, MCM v3 (Part B): tropospheric degradation of aromatic volatile organic compounds. *Atmospheric Chemistry and Physics*, 3(1):181–193, 2003.

18

T. R. Karl and K. E. Trenberth. Modern global climate change. *Science*, 302(5651):1719–1723, 2003.

L. I. Kleinman. The dependence of tropospheric ozone production rate on ozone precursors. *Atmospheric Environment*, 39(3):575 – 586, 2005.

J. J. P. Kuenen, A. J. H. Visschedijk, M. Jozwicka, and H. A. C. Denier van der Gon. TNO-MACC_II emission inventory; a multi-year (2003–2009) consistent high-resolution european emission inventory for air quality modelling. *Atmospheric Chemistry and Physics*, 14(20): 10963–10976, 2014.

K. A. Mar, N. Ojha, A. Pozzer, and T. M. Butler. WRF-Chem Simulations over Europe: Model Evaluation and Chemical Mechanism Comparison. *In Preparation*, 2016.

R. Mészáros, I. G. Zsély, D. Szinyei, C. Vincze, and I. Lagzi. Sensitivity analysis of an ozone deposition model. *Atmospheric Environment*, 43(3):663 – 672, 2009.

N. Otero, J. Sillmann, J. L. Schnell, H. W. Rust, and T. Butler. Synoptic and meteorological drivers of extreme ozone concentrations over europe. *Environmental Research Letters*, 11(2): 024005, 2016.

N. Passant. Speciation of UK emissions of non-methane volatile organic compounds. Technical report, DEFRA, Oxon, UK., 2002.

G. Pouliot, H. A. D. van der Gon, J. Kuenen, J. Zhang, M. D. Moran, and P. A. Makar. Analysis of the emission inventories and model-ready emission datasets of Europe and North America for phase 2 of the AQMEII project. *Atmospheric Environment*, 115:345–360, 2015.

S. E. Pusede, D. R. Gentner, P. J. Wooldridge, E. C. Browne, A. W. Rollins, K.-E. Min, A. R. Russell, J. Thomas, L. Zhang, W. H. Brune, S. B. Henry, J. P. DiGangi, F. N. Keutsch, S. A. Harrold, J. A. Thornton, M. R. Beaver, J. M. St. Clair, P. O. Wennberg, J. Sanders, X. Ren, T. C. VandenBoer, M. Z. Markovic, A. Guha, R. Weber, A. H. Goldstein, and R. C. Cohen. On the temperature dependence of organic reactivity, nitrogen oxides, ozone production, and the impact of emission controls in San Joaquin Valley, California. *Atmospheric Chemistry and Physics*, 14(7):3373–3395, 2014.

S. E. Pusede, A. L. Steiner, and R. C. Cohen. Temperature and Recent Trends in the Chemistry of Continental Surface Ozone. *Chemical Reviews*, 115(10):3898–3918, 2015.

D. J. Rasmussen, J. Hu, A. Mahmud, and M. J. Kleeman. The ozone–climate penalty: Past, present, and future. *Environmental Science & Technology*, 47(24):14258–14266, 2013. PMID: 24187951.

A. Rickard, J. Young, M. J. Pilling, M. E. Jenkin, S. Pascoe, and S. M. Saunders. The Master Chemical Mechanism Version MCM v3.2. `http://mcm.leeds.ac.uk/MCMv3.2/`, 2015. [Online; accessed 25-March-2015].

J. I. Rubin, A. J. Kean, R. A. Harley, D. B. Millet, and A. H. Goldstein. Temperature dependence of volatile organic compound evaporative emissions from motor vehicles. *Journal of Geophysical Research: Atmospheres*, 111(D3), 2006. D03305.

Y. Sadanaga, A. Yoshino, S. Kato, , and Y. Kajii. Measurements of oh reactivity and photochemical ozone production in the urban atmosphere. *Environmental Science & Technology*, 39(22):8847–8852, 2005. PMID: 16323785.

R. Sander, A. Kerkweg, P. Jöckel, and J. Lelieveld. Technical note: The new comprehensive atmospheric chemistry module mecca. *Atmospheric Chemistry and Physics*, 5(2):445–450, 2005.

S. M. Saunders, M. E. Jenkin, R. G. Derwent, and M. J. Pilling. Protocol for the development of the Master Chemical Mechanism, MCM v3 (Part A): tropospheric degradation of non-aromatic volatile organic compounds. *Atmospheric Chemistry and Physics*, 3(1):161–180, 2003.

J. L. Schnell, M. J. Prather, B. Josse, V. Naik, L. W. Horowitz, P. Cameron-Smith, D. Bergmann, G. Zeng, D. A. Plummer, K. Sudo, T. Nagashima, D. T. Shindell, G. Faluvegi, and S. A. Strode. Use of north american and european air quality networks to evaluate global chemistry–climate modeling of surface ozone. *Atmospheric Chemistry and Physics*, 15(18):10581–10596, 2015.

S. Sillman. The use of NOy, H2O2, and HNO3 as indicators for ozone-NOx-hydrocarbon sensitivity in urban locations. *Journal of Geophysical Research: Atmospheres*, 100(D7):14175–14188, 1995.

S. Sillman. The relation between ozone, NOx and hydrocarbons in urban and polluted rural environments. *Atmospheric Environment*, 33(12):1821 – 1845, 1999.

S. Sillman and P. J. Samson. Impact of temperature on oxidant photochemistry in urban, polluted rural and remote environments. *Journal of Geophysical Research: Atmospheres*, 100 (D6):11497–11508, 1995.

D. Simpson, A. Benedictow, H. Berge, R. Bergström, L. D. Emberson, H. Fagerli, C. R. Flechard, G. D. Hayman, M. Gauss, J. E. Jonson, M. E. Jenkin, A. Nyíri, C. Richter, V. S. Semeena, S. Tsyro, J.-P. Tuovinen, Á. Valdebenito, and P. Wind. The EMEP MSC-W chemical transport model – technical description. *Atmospheric Chemistry and Physics*, 12(16):7825–7865, 2012.

A. L. Steiner, S. Tonse, R. C. Cohen, A. H. Goldstein, and R. A. Harley. Influence of future climate and emissions on regional air quality in California. *Journal of Geophysical Research: Atmospheres*, 111(D18), 2006. D18303.

W. R. Stockwell, P. Middleton, J. S. Chang, and X. Tang. The second generation regional acid deposition model chemical mechanism for regional air quality modeling. *Journal of Geophysical Research: Atmospheres*, 95(D10):16343–16367, 1990.

W. R. Stockwell, F. Kirchner, M. Kuhn, and S. Seefeld. A new mechanism for regional atmospheric chemistry modeling. *Journal of Geophysical Research: Atmospheres*, 102(D22):25847–25879, 1997.

E. von Schneidemesser, P. S. Monks, J. D. Allan, L. Bruhwiler, P. Forster, D. Fowler, A. Lauer, W. T. Morgan, P. Paasonen, M. Righi, K. Sindelarova, and M. A. Sutton. Chemistry and the Linkages between Air Quality and Climate Change. *Chemical Reviews*, 2015. PMID: 25926133.

E. von Schneidemesser, J. Coates, A. J. H. Visschedijk, H. A. C. Denier van der Gon, and T. M. Butler. Variation of the NMVOC speciation in the solvent sector and the sensitivity of modelled tropospheric ozone. *Atmospheric Environment*, Submitted for Publication, 2016.

P. Wagner and W. Kuttler. Biogenic and anthropogenic isoprene in the near-surface urban atmosphere — A case study in Essen, Germany. *Science of The Total Environment*, 475:104 – 115, 2014.

G. Yarwood, S. Rao, M. Yocke, and G. Z. Whitten. Updates to the Carbon Bond Chemical Mechanism: CB05. Technical report, U. S Environmental Protection Agency, 2005.